SF2A 2013
L. Cambrésy, F. Martins, E. Nuss and A. Palacios (eds)

WEB-BASED SCIENTIFIC SIMULATION TOOLS FOR E-ELT INSTRUMENTS

K. Disseau[1], M. Puech [1], Y.B. Yang[1], H. Flores[1], F. Hammer[1] and L. Pentericci[2]

Abstract. In the frame of the EAGLE & OPTIMOS-EVE phase A studies, we have developped a scientific simulator which has been used to constrain the instrument high level specifications. The simulator is coupled to a web interface to allow an easier access by the science teams and run specific simulations covering the scientific objectives. This simulator is now used to constrain the design of MOSAIC, a new MOS concept for the E-ELT. We give a functional description of the simulator and illustrate how it is used in practice to constrain the pixel size of the IFU of MOSAIC.

Keywords: 3D spectroscopy, Integral field spectroscopy, Simulations, Imagery, ELTs

1 Introduction

In the frame of the ESO E-ELT instrument phase A studies (Puech et al. (2008), Evans et al. (2011), Navarro et al. (2010), Puech et al. (2010)), we have developped a scientific simulator coupled to a web interface. It is now used to constrain the MOSAIC design (Hammer et al., these proceedings). We also developped other telescope/instrument simulators, including a general image/datacube simulator which is acessible at `https://websim.obspm.fr`. After a functional description of the simulator we illustrate its use to constrain the IFU pixel size of MOSAIC in the detection of UV interstellar absorption lines and the Ly-α emission line in high redshift galaxies.

2 Methodology

This end-to-end simulator produces datacubes in FITS format, mimicking the result of real observations. An AO system can be modeled through its PSF, which is simulated using a dedicated pipeline not included in this simulator. Iterative simulations allow to converge toward a science versus technique trade-off.
The simulator is coupled to a web interface hosted on a secured server called WEBSIM, and the simulations are run on a science server. When completed, an email is sent to the user who can then download the products consisting in FITS files. The user can choose through this interface the instrument characteristics, such as the IFU size, the spectral resolution, the CCD performances etc, and also the scientific target among several available templates. AO correction of atmospheric turbulence is set through the choice of the PSF (see Fig. 1). Details can be found in Puech et al. (2010)

3 Developments

Updates of this simulator are planned over the next two years, including the implementation of temporal and spatial sky background variations, thanks to the work that has been done in our team to better understand the sky background variations and to develop techniques to properly substract it (Yang et al. (2013)). It is also planned to include telluric features and to implement a batch mode to run several simulations in a row. Moreover, a complete AO PSF library will be offered (LTAO, MCAO, MOAO, XAO) as well as morpho-kinematic templates for simulating a large range of astrophysical objects of interest. This will be done in the frame of the COMPASS project (PI : D. Gratadour), founded by the French ANR.

[1] GEPI, Observatoire de Paris, CNRS, Université Paris-Diderot; 5 place Jules Janssen, 92190 Meudon, France
[2] INAF, Osservatori Astronomico di Roma, via Frascati 33, 00040 Monte Porzio Catone, Italy

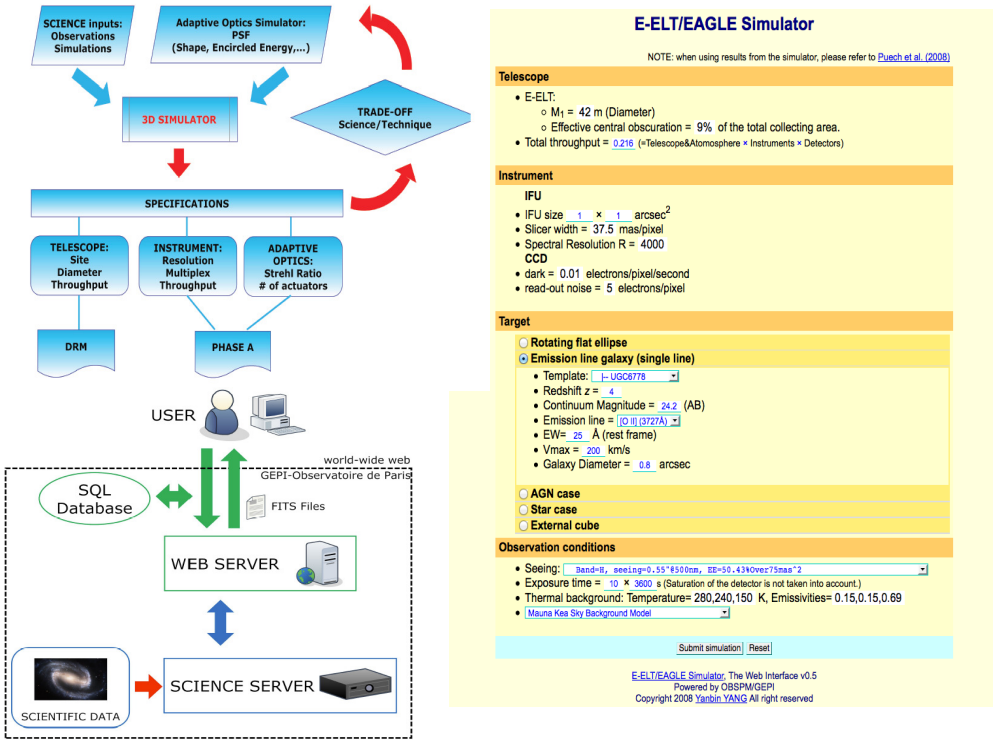

Fig. 1. Left upper pannel: Schematic illustration of the use of simulations to constrain telescope or instrument specifications. **Left bottom pannel :** Overall structure of WEBSIM. **Right pannel:** Web interface of the simulator.

4 Simulations

We considered in these simulations a 39-m diameter telescope with a 11-m secondary mirror. We used an MOAO PSF from EAGLE phase A study which provides 30% of ensquared energy in 80×80 mas^2, and we assumed a spectral resolution $R = 4000$, which is the minimum required to target emission lines between the OH sky lines and to resolve Ly-α profiles with typical FWHM∼150-500 km/s. These simulations aimed at constraining the optimal pixel scale ; we thus simulated different sizes of pixels, from 20 mas to 900 mas. Once the resulting datacubes simulated, we analysed them by constructing integrated spectra following Rosales-Ortega et al. (2012) (see their Fig.2) : spectra are added by order of decreasing S/N until the S/N of the integrated spectrum stops increasing.

4.1 Simulated IFU observations of UV interstellar lines at $z \sim 7$

The spatial distribution of the light is based on hydrodynamical simulations of clumpy disks by Bournaud et al. (2007), which have been rescaled in flux and sizes to observations at $z = 7$. We simulated a range of object apparent magnitudes from $J_{AB} = 25$ to $J_{AB} = 28$. Following the distribution of half light radii of LBG galaxies observed with HST (Grazian et al. (2012)), we assumed three typical sizes for the simulated galaxies : a compact size (R_{half}=100 mas), an average size (R_{half}=150 mas) and a large size (R_{half}=210 mas). Behind each spaxel of the cube is attached a template LBG spectrum from Shapley et al. (2003) resampled at $R = 4000$. The analysis of integrated spectra (illustrated in Fig. 2 and Fig. 3) shows that J_{AB}=26-27 should be detected with t_{intg}=40 hrs and a 80 mas pixel scale, for which the S/N is maximum. Below 80 mas it is limited by the readout noise and above 120 mas by the sky background.

4.2 Simulated IFU observations of Ly-α emission line at $z \sim 9$

The spatial distrubution of light is the same as for UV lines case. The simulated grid was extended to fainter magnitudes (up to $J_{AB} = 30$). Following current observations of LAEs at $z \sim 6$, we modeled the Ly-α line

with a gaussian line truncated in the blue side and with a width of 270 km/s ; we considered also a constant velocity field of 200 km/s (Swinbank et al. (2007)) mimicking a constant outflow. We increased the equivalent width with magnitude, according to data from Jiang et al. (2013) (see their Fig. 6). The results are shown in Fig. 2. The maximal S/N is obtained for pixel sizes ranging between 40 and 120 mas. There is no prefered value in this range since variations of S/N can be easily compensated by variations in integration time in this case. Simulations show that J_{AB}=30 should be easily detected with such pixel scales and with t_{intg}=10hrs (see Fig. 3).

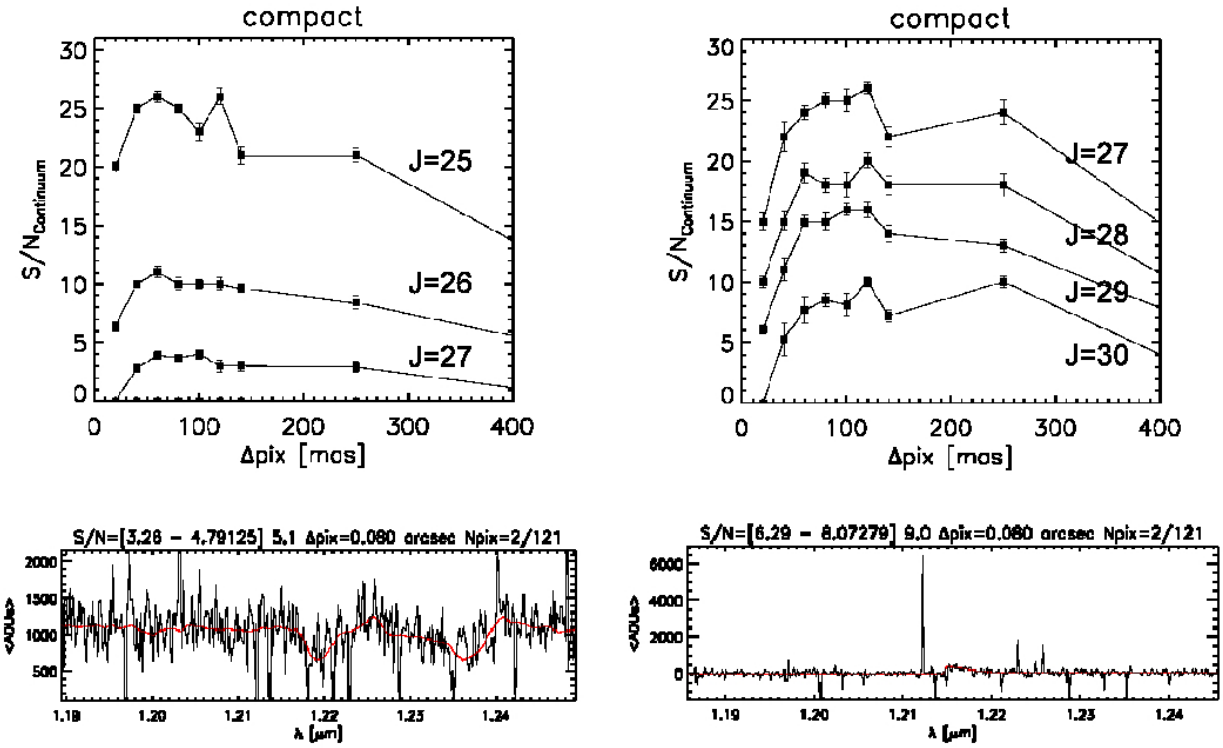

Fig. 2. Left : Simulated IFU observations of UV interstellar absorption lines at $z \sim 7$ with t_{intg}=40hrs on source. The top pannel shows the S/N in the SiII(λ=1527A) absorption line from integrated spectra of compact sources as a function of the IFU pixel size for different object apparent magnitudes. An exemple of such an integrated spectrum is given for J_{AB}=27 and 80 mas/pixel. The range of S/N in the line for the spectra used to construct the combined spectrum are shown in parentheses at the upper left of the spectrum, followed by the S/N of the integrated spectrum itself. **Right :** Simulated IFU observations of Lyman-α emitters redshifted to $z \sim 9$ with t_{intg}=10hrs on source. The S/N plotted in the top pannel is calculated in the Ly-α line. The bottom pannel shows an example of integrated spectrum for a compact source with J_{AB}=29 and 80 mas/pixel.

5 Conclusion

We used WEBSIM to constrain the high level specifications of MOSAIC, especially the IFU pixel scale. We found in the case of observing high redshift galaxies that the more dimensioning case is the study of interstellar UV lines, with a 80 mas pixel scale favored to reach $J_{AB} \sim 27$, assuming 40 hr integration time and a MOAO system delivering an Ensquared Energy of 30% within 80×80 mas^2. Deep LAEs spectra should be obtained with 40-120 mas IFUs and 10 hr integration time, up to $J_{AB} \sim 30$. The next step will consist in simulating the detection of LBGs and LAEs with GLAO-fed fibers in order to compare the performance with IFU integrated spectra.

These simulations will also be repeated with new AO PSFs that will be provided in the frame of COMPASS project, to determine whether the AO system can be simplified without degrading the instrument performances.

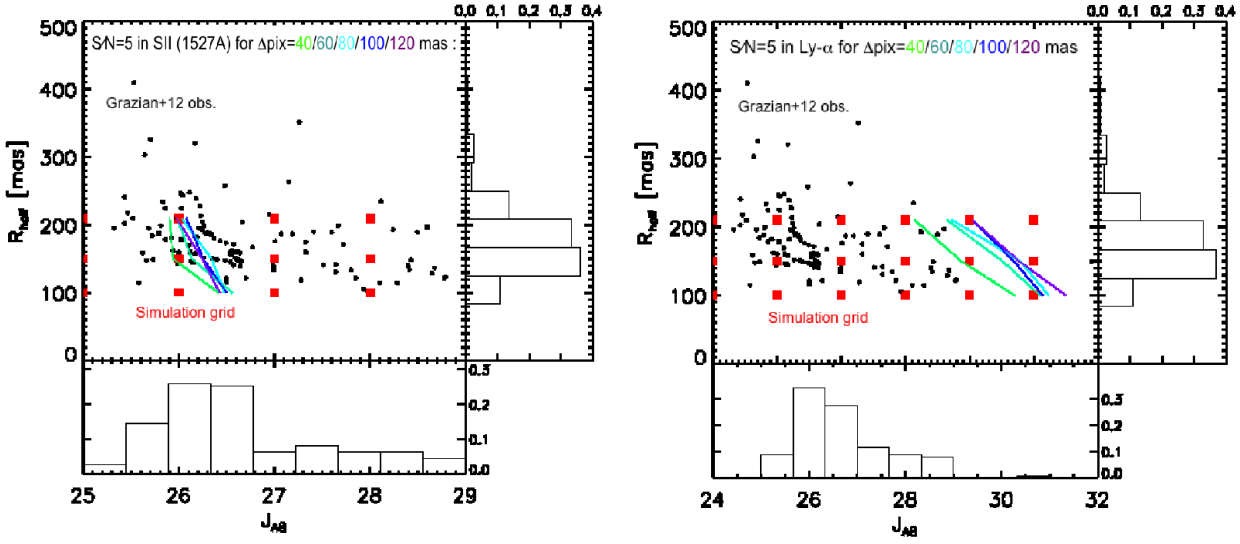

Fig. 3. Observed J_{AB} vs R_{half} distribution of $z \sim 7$ galaxy candidates. Simulated observations are indicated as red squares. The color lines show the limit at which S/N=5 is reached for each simulated pixel size. **Left:** Results for UV absorption lines simulations with t_{intg} =40 hrs. **Right:** Results for LAE simulations with t_{intg} =10 hrs.

References

Bournaud, F., Elmegreen, B.G., Elmegreen, D.M. 2007, ApJ, 670, 237
Evans, C. et al. 2011, A&A, 527, 50
Grazian, A. et al. 2012, A&A, 547,51
Jiang, L. et al. 2013, ApJ, 772, 99
Navarro, R. et al. 2010, SPIE 7735, 88
Puech, M. et al. 2008, MNRAS, 390, 1089
Puech, M. et al. 2010, MNRAS 402, 903
Puech, M., Yang, Y.B., Flores, H. SPIE 7735, 183
Rosales-Ortega, F.F, Arribas, S., Colina, L. 2012, A&A 539, 73
Shapley, A., Steidel, C., Pettini, M. and Adelberger, K. 2003, ApJ, 588, 65
Swinbank, A.M. et al. 2007, MNRAS, 376, 479
Yang, Y.B. et al. 2013, The ESO Messenger, 151, 10